arXiv:1408.4884v1 [nucl-th] 21 Aug 2014

Electron capture strength on odd-A nucleus ^{59}Co in explosive astrophysical environment

Muneeb-Ur Rahman[1] • **Jameel-Un Nabi**[2]

Abstract The Gamow-Teller (GT) transitions within massive stars play sumptuous role in the dynamics of core collapse supernovae. GT strength distributions and electron capture rates have been calculated for odd-A nucleus ^{59}Co within the proton-neutron quasiparticles random phase approximation (pn-QRPA) formalism. The pn-QRPA results are compared with other model calculations and (n, p) reaction experiment carried out at TRIUMF charge-exchange facility. The pn-QRPA calculated a total $B(GT_+)$ strength of 3.3 for ^{59}Co to be compared with the shell model value of 2.5 and the 1.9 ± 0.1 in the (n, p) charge-exchange reaction. Aufderheide et. al. (1) extracted total strength equaling 2.4 ± 0.3. The placement of GT centroid at 5.6 MeV by the pn-QRPA model is in reasonable agreement with the shell model centroid at 5.1 MeV whereas the measured GT centroid was placed at 4.4 ± 0.3 MeV in the (n, p) experiment. Fuller, Fowler and Newman (FFN) (2; 3; 4), placed the GT centroid at too low excitation energy of 2.0 MeV in the daughter nucleus ^{59}Fe, and this misplacement led to the enhancement of FFN rates. The suppressed pn-QRPA and shell model electron capture rates are in good agreement with each other. The rates are suggestive of higher value of Y_e (electron-to-baryon ratio) and may contribute to a more massive homologously collapsing core resulting in a more energetic shock. It might be interesting for the simulators to check the effect of these suppressed rates on the fine-tuning of the time rate of Y_e, the concomitant heavy element nucleosynthesis, and, on the energetics of the subsequent shock wave.

Keywords Gamow-Teller (GT) strength distribution; GT centroid; electron capture; pn-QRPA; stellar dynamics; core-collapse.

Muneeb-Ur Rahman

Department of Physics, Islamia College Peshawar, KPK, Pakistan
email: muneeb@icp.edu.pk

Jameel-Un Nabi

Faculty of Engineering Sciences, GIK Institute of Engineering Sciences and Technology, Topi 23640, Swabi, KPK, Pakistan
email: jameel@giki.edu.pk

1 Introduction

Supernovae (either type-Ia or type-II) are very crucial to our very existence as well as the structural and morphological development of the galaxies and universe at large. These two types of supernovae are the major contributors for the elements production in the universe. Iron in the universe is made approximately in equal amount by type-Ia and type-II supernovae (5). The incarnation of these supernovae starts when the mass of the iron core exceeds the appropriate Chandrasekhar mass limit. The electron degeneracy pressure is no longer in a position to sustain the inner core against the gravitational collapse. Consequently the implosion ensues and leads to a more exotic and denser matter. A smaller entropy as well as a smaller iron core mass favor the explosion mechanism as the shock has to plough a little mass of the inner core. The shock wave looses less energy in the photodisintegration process and the lower entropy helps in the reduction of free protons in stellar matter which in turn reduces the probability of electron capture rates on free protons and thus leads to a higher value of Y_e (lepton-to-baryon ratio) at the bounce.

The mass of the homologous collapsing core and subsequent shock is determined by final value of the Y_e of the stellar core. The mass of the homologous collapsing core is related to the final lepton number as $M_{hc} \propto Y_{ef}^2$. When the core stiffens beyond the nuclear density it sends an outward shock wave with energy:

$$E_S \simeq (GM_{HC}^2/R_{HC})(Y_{ef} - Y_{ei}) \quad (1)$$
$$\simeq M_{HC}^{5/3}(Y_{ef} - Y_{ei}) \simeq Y_{ef}^{10/3}(Y_{ef} - Y_{ei}),$$

disintegrating the stellar matter (6). Where M_{HC}, R_{HC} are the mass and radius of the homologous core, respectively. The energy of the shock is larger for larger difference of initial and final lepton fractions and for larger final lepton fraction prior to collapse. Weak decay rates, such as electron/positron captures and $\beta^{\pm}$ decays, affect the central lepton fraction Y_e, which subsequently determines the composition of the ejecta from supernova explosions (7; 8; 9). Iron group nuclei have highest binding energy and element synthesis beyond the iron group nuclei in the stellar kiln is energetically not possible. Consequently the star's energy budget and electron degeneracy pressure are unable to counter the mammoth inward gravitational force. The density and temperature of the stellar core increase with further addition of mass and this leads the core to reduce its free energy via electron capture process on protons in the nuclei and reduces the Y_e at initial stage of the collapse (10). The concomitant nucleosynthesis via electron capture change the Y_e and consequently the composition of matter in astrophysical scenario. At this stage, when the density is not high enough ($\leq 10^{10}$ g/cm^3), the neutrinos bleed out from the star carrying along enormous amount of energy. Both neutrino bleeding and reduction in Y_e accelerate the collapse process. This collapse of the star is very sensitive to the entropy and to the number of leptons per baryon, Y_e (9; 11; 12; 13).

Bethe and collaborators (11) investigated, for the first time, the importance of Gamow-Teller (GT) transitions for the stellar weak decay rates. The GT transitions are one of the most essential and paramount nuclear weak processes of the spin-isospin ($\sigma\tau$) type and are involved actively in various processes such as nucleosynthesis and stellar core collapse of massive stars preceding supernova explosions. Later Fuller, Fowler, and Newman (2; 3; 4) (referred to as FFN in this paper) investigated the GT transitions and calculated the weak decay rates for 226 nuclei in the mass range 21 $\leq A \leq$ 60 at densities and temperatures pertinent to astrophysical environment using parameterization based on independent particle model. For unmeasured GT transition of allowed nature, they assumed an empirical value of logft = 5. FFN employed the so-called Brink's hypothesis in their calculations. This hypothesis assumes that the GT strength distributions on the excited states are the same as that on the ground state shifted only by the excitation energy of that particular excited state (see Ref. (14) for further details). Brink's hypothesis was later found to be a poor approximation to be employed in stellar weak interaction rate calculations (9; 12; 13; 15; 16; 17). Charge-exchange reactions, such as (p, n) and (n, p) experiments, confirm the misplacement of GT centroid in FFN's calculations and it was further observed that GT strength is quenched and fragmented. These developments led the scientific community to use microscopic approaches for a reliable calculation of stellar weak decay rates.

Large-scale shell model (18) and proton-neutron quasiparticle random phase approximation (pn-QRPA) theory (19) are two such microscopic models used with relative success for a reliable calculation of stellar weak decay rates. Both microscopic models have associated pros and cons. In shell model emphasis is more on interactions as compared to correlations whereas pn-QRPA puts more weight in correlations. It is difficult to comment which method should suit the notoriously complex dynamics of core collapse. The shell model Monte Carlo (SMMC) techniques (e.g. Ref. (20)) were also used for the calculations of the GT strength distributions in pf-shell nuclei with associated pros and cons. SMMC does not allow for detailed nuclear spectroscopy and has some restrictions in its applications for odd-A and odd-odd nuclei. It has also been noted that the SMMC's average GT strength distribution introduces inaccuracies in the weak decay rates calculations (21). Different calculations of GT strength distributions and weak decay rates are now available, and can be found in literature (e.g. (9; 15; 19; 21; 22; 23; 24; 25)).

Electron capture rate on ^{59}Co is argued to play a pivotal role in the presupernova evolution of massive stars (e.g. see the simulation results of Refs. (24; 26). In this paper we used the pn-QRPA theory to calculate the GT strength distributions and weak decay rates for the odd mass nucleus, ^{59}Co, at densities and temperature relevant for pre-collapse and supernova phases of massive stars.

The paper is organized as follows. Section 2 describes the theoretical formalism used for the calculation of $B(GT_+)$ strength and weak decay rates based on pn-QRPA model. The calculated GT strength for ^{59}Co is presented in Section 3. Here we also present comparisons with the (n, p) experiment and previous calculations. The calculated electron capture rates are presented in Section 4. We finally conclude our findings in Section 5.

2 Formalism

The electron capture rates (Z, A) + e $\rightarrow$ (Z-1, A) + ν mediated by charged weak interaction are calculated

within the domain of pn-QRPA model. The pn-QRPA is considered to be an efficient model to extract the GT strength distributions for ground as well as excited states of the nuclei present in stellar matter (19; 27). During pre-collapse and supernova phases of massive stars, transitions from excited states contribute effectively to the total electron capture rate and a microscopic calculation of *all* excited state GT strength distributions is desirable. The pn-QRPA model is used in the present work to calculate the $B(GT_+)$ strength distribution and associated electron capture rates on odd-A nucleus ^{59}Co using a luxurious model space of $7\hbar\omega$. The model is capable of performing a microscopic calculation of ground *and* excited states GT strength distribution functions.

The Hamiltonian used in our calculation had four parts and is of the form

$$\mathrm{H^{QRPA}} = \mathrm{H^{sp}} + \mathrm{V^{pair}} + \mathrm{V^{ph}_{GT}} + \mathrm{V^{pp}_{GT}}, \quad (2)$$

where H^{sp}, V^{pair}, V^{ph}_{GT}, V^{pp}_{GT} are the single-particle Hamiltonian, the pairing force, the particle-hole (ph) GT force, and the particle-particle (pp) GT force, respectively. In the present work, in addition to the well known particle-hole GT force (28; 29; 30), the particle-particle GT force (31; 32) is also taken into account. The electron capture rate of a transition from the ith state of a parent nucleus (Z, N) to the jth state of the daughter nucleus $(Z-1, N+1)$ is given by

$$\lambda^{ec}_{ij} = \ln 2 \frac{f_{ij}(T,\rho,E_f)}{(ft)_{ij}}. \quad (3)$$

The $(ft)_{ij}$ of an ordinary $\beta^{\pm}$ decay from the state $|i\rangle$ of the parent nucleus to the state $|f\rangle$ of the daughter is related to the reduced transition probability B_{ij} of the nuclear transition by

$$(ft)_{ij} = D/B_{ij}. \quad (4)$$

The value of D is taken to be 6146 $\pm$ 6 s adopted from Ref. (33), and B_{ij} is given by

$$B_{ij} = B(F)_{ij} + (g_A/g_V)^2_{\mathit{eff}} B(GT)_{ij}. \quad (5)$$

Here $B(F)_{ij}$ and $B(GT)_{ij}$ are the reduced transition probabilities due to Fermi and GT transitions and $(g_A/g_V)^2_{\mathit{eff}}$ is the effective ratio of the axial-vector (g_A) to the vector (g_V) coupling constants that takes into account the observed quenching of the GT strength (34). In the present work $(g_A/g_V)_{\mathit{eff}}$ was taken as

$$(g_A/g_V)^2_{\mathit{eff}} = 0.66\,(g_A/g_V)^2_{\mathit{bare}} \quad (6)$$

with $(g_A/g_V)_{\mathit{bare}}$ taken as -1.257.

The phase space integrals are

$$f_{ij} = \int_{w_l}^{\infty} w\sqrt{w^2-1}(w_m + w)^2 F(+Z,w) G_- dw, \quad (7)$$

where G_- is the electron distribution function. $F(+z,w)$ are the so-called Fermi functions and are calculated according to the procedure adopted by Ref. (35). In Eq. 7 energies are given in units of $m_e c^2$ and momenta in units of $m_e c$. In Eq. 7, w is the total energy of the electron including its rest mass, w_l is the total capture threshold energy (rest + kinetic) for electron capture. One should note that if the corresponding positron emission total energy, w_m, is greater than -1, then $w_l = 1$, and if it is less than or equal to 1, then $w_l = \mid w_m \mid$. w_m is the total β-decay energy in units of $m_e c^2$,

$$w_m = \frac{1}{m_e c^2}(m_p - m_d + E_i - E_j), \quad (8)$$

where m_p and E_i are mass and excitation energies of the parent nucleus, and m_d and E_j of the daughter nucleus, respectively.

The number density of electrons associated with protons and nuclei is $\rho Y_e N_A$, where ρ is the baryon density, Y_e is the ratio of electron number to the baryon number, and N_A is the Avogadro's number.

$$\rho Y_e = \frac{1}{\pi^2 N_A}\left(\frac{m_e c}{\hbar}\right)^3 \int_0^{\infty} (G_- - G_+) p^2 dp, \quad (9)$$

where $p = (w^2-1)^{1/2}$ is the electron or positron momentum in units of $m_e c$ and G_+ is the positron distribution function. The neutrino blocking of the phase space is not taken into account. We assume that neutrinos and antineutrinos escape freely from the interior of the star under prevailing physical conditions. The total electron capture rate per unit time for a nucleus in thermal equilibrium at temperature T is finally achieved by performing a summation over all partial rates and is given by

$$\lambda_{ec} = \sum_{ij} P_i \lambda^{ec}_{ij}. \quad (10)$$

Here P_i is the probability of occupation of parent excited states and follows the normal Boltzmann distribution. The summation in Eq. 9 is carried out over all initial and final states until satisfactory convergence in the rate calculations is achieved.

3 Comparison of Gamow-Teller Strength Distributions for ^{59}Co

The *fp*-shell nucleus ^{59}Co, akin to ^{51}V, is considered to play a significant role in the late stages just prior to the presupernova collapse of the stellar core in massive stars (24; 26; 36). They used the iron-group nuclei, including $^{44-52}$Ti, $^{47-54}$V and $^{54-64}$Co, $^{56-66}$Ni, to calculate abundances in nuclear equilibrium and stressed that this group of nuclei should be adequate to represent the electron capture and beta decay processes for stellar core having $Y_e \gtrsim 0.43$. The cross section for GT transitions is directly proportional to the cross section of electron capture on nuclei (37) and is considered as important essence in the simulation of core collapse of heavy mass stars (2; 3; 14). In this section we report the pn-QRPA calculation for the $B(GT_+)$ strength distribution of ^{59}Co. The experimental data extracted in charge-exchange reactions show that the GT strength is strongly quenched as compared to the independent model value and is fragmented over many states in the daughter nucleus (e.g. (36; 38)). For the case of ^{59}Co, the pn-QRPA GT strengths were renormalized with a quenching factor of 0.66 (see Eq. 6). The pn-QRPA calculated $B(GT_+)$ results and it's comparison with the observed GT strength function measured in the (n, p) reaction carried out using TRIUMF charge-exchange facility (39) is shown in Fig. 1. On the other hand Fig. 2 displays a mutual comparison between the pn-QRPA and shell model GT strength calculation (21). In both figures the vertical axis shows $B(GT_+)$ strength in arbitrary units whereas the horizontal axis represents the excitation energy in daughter nucleus, ^{59}Fe, in units of MeV. The authors in (39) also carried out a shell model calculation in truncated model spaces and employed a renormalization factor of 0.24 to compare the theoretical strength with the experimental (n, p) data. The shell model rates, performed in one major shell, in Ref. (21) also incorporated a quenching factor of 0.74 in their calculation.

The over all morphology of pn-QRPA calculated GT strength distribution is satisfactory except in the high energy region when compared with the measured strength. Both the pn-QRPA and shell model predict very little strength above 8 MeV as compared to measured strength. The pn-QRPA extracted a total strength of 3.32 for ^{59}Co. The total strength observed in the (n, p) reaction is 1.9 ± 0.1 units for ^{59}Co (39) whereas shell model calculated a total value of 2.5 (21). The authors in Ref. (1) quoted a total GT strength of 2.4 ± 0.3 for ^{59}Co. The pn-QRPA placed the GT centroid at 5.6 MeV, which is in reasonable agreement with the shell model centroid placement at 5.05 MeV (21). FFN (2; 3; 4) assumed that almost all the GT strength is concentrated in a collective state also referred to as GT resonance (GTR). FFN lodged the GT resonance at too low excitation energy of 2.00 MeV in daughter ^{59}Fe. For further details of misplacement of GT centroid in FFN calculation we refer to (21). The placement of GTR by FFN is shown by an arrow in Fig. 1 and Fig. 2. The measured GT centroid in the charge-exchange (n, p) reaction (39) resides at an excitation energy of 4.4 ± 0.3 MeV in the daughter ^{59}Fe. The pn-QRPA calculated GT centroids and integrated GT strengths for odd A nuclei, ^{59}Co and ^{51}V, along the electron capture direction, are compared with other model calculations and experiments in Table 1.

4 Electron Capture Rates on ^{59}Co

The stellar electron capture rates on ^{59}Co were calculated within the pn-QRPA formalism for temperature and density grid relevant to pre-collapse and supernova phases of massive stars. The mass compilation of Audi and collaborators (40; 41) was used to calculate Q-value of the reaction. The reported pn-QRPA rates for ^{59}Co are compared with large scale shell model rates (18) and those performed by FFN (2; 3; 4) in Fig. 3. Here the vertical axis represent the calculated electron capture rates in units of s^{-1}. It is noted that the capture rates are plotted on a logarithmic scale (to base 10). Stellar temperature T_9 is shown on the horizontal axis where T_9 represents the temperature in units of $10^9 K$. The pn-QRPA model calculated a much bigger value of the total GT strength when compared with the shell model calculation (see Table 1). Correspondingly the shell model rates are smaller by a factor 8 to 20 than the pn-QRPA rates in the stellar core when encountering a low temperature and density environment. The microscopic calculation of GT strength of low-lying states guarantees a reliable description of the weak rates at low temperatures and/or densities (18), where the individual transitions play preeminent role in the capture processes. As the temperature of the stellar core increases the shell model rates approaches the pn-QRPA rates. For ^{59}Co, the pn-QRPA placed the GT centroid at an energy 0.5 MeV higher than the shell model centroid in daughter ^{59}Fe. This low centroid placement by shell model effectively contributes to the enhancement of shell model capture rates at higher temperatures. The stellar weak rates are one of the most important nuclear physics input parameters for simulation of core collapse. Yet the uncertainty involved in their calculation is considerable. What the simulators require is a reliable calculation of these rates on

a detailed temperature-density scale pertinent to the presupernova and supernova environments. Both shell model and pn-QRPA calculations do employ certain approximations at various stages of their calculation and as such the total stellar electron capture rates do differ. These small differences provide reliable alternatives to the simulators to model a mere 1% effect (we recall that $< 1\%$ of the gravitational binding energy of the star goes into the kinetic energy of the ejected envelope). Calculations by Burrows and Sawyer (42) do show that correlations significantly reduce neutrino opacity, making more energy available to be carried to the envelope.

The pn-QRPA electron capture rates for ^{59}Co are also compared with the FFN rate calculations in Fig. 3. It can be seen from the figure that the pn-QRPA rates are enhanced at $T_9 = 1$ for low densities 10^3 g/cm^3 and 10^7 g/cm^3. At low densities the capture rates are sensitive to the details of GT strength distributions. FFN employ a phenomenological calculation and did not employ any microscopic approach to calculate the GT strength functions from the excited states. Moreover FFN used the Brink's hypothesis (as discussed earlier) in their calculations (also employed by large scale shell model calculation). At higher temperatures the FFN rates get enhanced in comparison to the pn-QRPA rates. As temperature rises the probability of occupation of the parent excited states increases and in the FFN calculations the parent excitation energies were not constrained (by particle emission processes) and this resulted in an enhancement in their capture rates at higher temperatures. FFN did not take into account the particle emission processes from higher excited states. As a result the parent excited states (and resulting GT transitions using Brink's hypothesis) extended well beyond particle emission threshold energies. These states had a finite occupation probability at high temperatures and consequently significant contribution to total electron capture rates as can be seen from Eq. 10. Another reason for enhancement in the capture rates of FFN is due to the placement of GT centroid at too low energy of 2.00 MeV in daughter nucleus (for details see Refs. (18; 21; 43)). In high density region ($\sim 10^{11}$ g/cm^3) the FFN rates are bigger by roughly an order of magnitude for all temperature ranges for reasons already mentioned.

5 Discussion and Conclusions

The aim of the present work was to calculate the $B(GT_+)$ strength distribution and associated electron capture rates, at densities and temperatures that are relevant to explosive stellar environment, for the key fp-shell nucleus ^{59}Co. The GT transitions largely determine electron capture rates which play a decisive role and used as a vital input parameter in the simulations codes of core collapse of massive stars. Consequently GT strength is an important ingredient related to the complex dynamics of presupernova and supernova explosion. The $B(GT_+)$ strength distribution for odd-A ^{59}Co nucleus was calculated using the pn-QRPA theory with a model space of $7\hbar\omega$. The comparison of the pn-QRPA model with experimental results of (n, p) reaction data, and with theoretical calculations of shell model and FFN was made. The total GT strength and the GT centroid calculated within the domain of pn-QRPA are in reasonable agreement with the experimental value and reported shell model values. FFN, on the other hand, placed the GT centroid at too low excitation energy of 2.00 MeV in daughter ^{59}Fe which resulted in artificial enhancement of their rates. The electron capture rates in stellar matter are sensitive to the location of GT centroid and GT strength distribution of these low-lying states in daughter ^{59}Fe. Consequently the FFN rates are enhanced both at low and high density regions in stellar matter. The FFN rates are also enhanced at higher temperatures. The reason for this enhancement in the FFN rates was that particle emission processes were neglected by FFN and as such there was no cutoff in FFN calculation for parent excitation energies. The partial capture rates from these high-lying excited states contributed to the total rates at high temperatures. Small changes in the binding and excitation energies can lead to significant modifications of the predictions for the synthesis of elements in the stellar kline. The good agreement of the low-lying pn-QRPA calculated GT strength with experimental results may affect the prediction and synthesis of ^{59}Fe as well as the evolution timescale and dynamics of the collapsing supermassive stars.

The calculated electron capture rates on ^{59}Co in stellar matter are in good agreement with the large scale shell model rates for all temperature range. Only at high density of around $\rho Y_e = 10^{11}$ g/cm^3 do the pn-QRPA rates get suppressed by a factor of two. The corresponding comparison with FFN rates is not as good and the pn-QRPA electron capture rates are suppressed by roughly an order of magnitude in high density region. Brachwitz et al. (7) performed model calculations for Type-Ia supernovae using FFN electron capture rates yielding overproduction of iron group nuclei. In order to investigate the soft X-ray emission of the magnetars with magnetic field strengths in excess of the quantum critical value $B_{cr} = 4.414 \times 10^{13} G$, Gao and collaborators (45; 46; 47; 48) simulated numerically the complete process of electron capture and

discussed its importance in the interior of the magnetars. Type-Ia supernovae are responsible for about half of the abundances of the iron-group nuclei in the galactic evolution (5). The authors in (49; 50) improved the previous weak decay rates evaluations by taking into account the electron screening corrections. They found that the capture rates get suppressed by an order of magnitude than those of FFN due to the inclusion of electron screening effect. The current suppressed electron capture rates suggest larger value of Y_e in the stellar cores. The higher the value of Y_e the larger will be the homologous core (see Eq. 1) which in turn affects the hydrodynamics at bounce and energy of the shock waves (51). Consequently, a prompt shock is created farther out with less overburden of heavier and tightly bound nuclei (52). This means that shock waves have to spend less energy in the dissociation of smaller iron core for outward march. Besides Y_e, the density just outside the iron core is also an important parameter which sets the "ram pressure" and the shock has to overcome it before generation of any successful supernova explosion. The density in this region is larger by as much as 50 percent and the new models find it challenging to produce a successful explosion (53). Notoriously enough the explosion mechanism does not depend on a single input parameter and requires data for a group of nuclei. The nucleosynthesis of the iron group and other nuclei strongly depend on many input parameters, e.g., the progenitor mass, mass cut, Y_e, explosion energy, mixing and fallback, metalicity of progenitor, energetics of shock, entropy of the core (54). It might be interesting for the simulators to study how the composition of the collapsing core and ejecta would be effected using the present and previously reported pn-QRPA electron capture rates and to compare the resulting simulation results with the observed abundances.

We are in a process to calculate GT_+ transitions and electron capture rates from ground and excited states of key *pf*-shell nuclei at densities and temperatures relevant to astrophysical scenario specially for which experimental data is either scarce or unavailable. The GT transitions from the excited states of the parent nuclei have finite contributions under prevailing physical conditions. It will be interesting to study the contribution of a microscopic calculation of GT strength distributions from these excited states on the total weak decay rates and its subsequent implication in simulation codes.

Acknowledgement: The authors would like to acknowledge the kind suggestions of the referee(s) which led to the correction in the formalism and overall improvement of the manuscript.

References

Aufderheide, M. B., Bloom, S. D., Resler, D. A., Mathews, G. J.: Shell-model calculations of Gamow-Teller strength in 51V, 54Fe, and 59Co. Phys. Rev. C **48**, 1677 (1993).

Fuller, G.M., Fowler, W.A., Newman, M.J.: Stellar Weak Interaction Rates for sd-shell Nuclei. I. Nuclear Matrix Element Systematics with Application to 26Al and Selected Nuclei of Importance to the Supernova Problem. Astrophys. J. Suppl. Ser.**42** 447(1980).

Fuller, G.M., Fowler, W.A., Newman, M.J.: Stellar Weak Interaction Rates for Intermediate-Mass Nuclei. III. Rate Tables for the Free Nucleons and Nuclei with A=21 to A=60. Astrophys. J. Suppl. Ser.**48**, 279(1982).

Fuller, G.M., Fowler, W.A., Newman, J.: Stellar Weak Interaction Rates for Intermediate-Mass Nuclei. II. A=21 to A=60. Astrophys. J. **252**, 715(1982).

Cowan J. J. and Thielemann F.-K.: R-process nucelosynthesis in supernovae. Phys. Today, October Issue, 47 (2004).

Kar, K., Ray, A., Sarkar, S.: Beta-Decay rates for *fp*-shell nuclei with A ¿ 60 in massive stars at the presupernova stage. The Astrophysical Journal **434**, 662-683 (1994).

Brachwitz, F., Dean, D.J., Hix, W.R., Iwamoto, K., Langanke, K., Martinez-Pinedo, G., Nomoto, K., Strayer, M.R., Thielemann, F-K., Umeda, H.: The Role of Electron Captures in Chandrasekhar-Mass Models for Type-Ia supernovae. The Astrophysical Journal **536**, 934-947 (2000).

Nabi, J.-U,: Ground and excited states Gamow-Teller strength distributions of iron isotopes and associated capture rates for core-collapse simulations. arXiv:1203.4675v1 [nucl-th] 21 Mar 2012.

Nabi, J.-U, Rahman, M.-U: Gamow-Teller strength distribution in proton-rich nucleus 57Zn and its implications in astrophysics. Astrophys Space Sci. **332**, 309317 (2011).

Langanke, K., Schatz, H.: The role of radioactive ion beams in nuclear astrophysics. Phys. Scr. **T152**, 014011 (2013).

Bethe, H. A., Brown, G. E., Applegate, J., Lattimer, J. M.: Equation of state in the gravitational collapse of stars. Nucl. Phys. A **324**, 487 (1979).

Nabi, J.-U, Rahman, M.-U: Gamow-Teller strength distributions and electron capture rates for 55Co and 56Ni. Phys. Lett. **B612**, 190-197 (2005).

Rahman, M.-U, Nabi, J.-U: The Nuclear Structure and Associated Electron Capture Rates on Odd-Z Nucleus ^{51}V in Stellar Matter. Astrophys. and Space Sci. DOI 10.1007/s10509-013-1580-5 (2013).

Aufderheide, M. B.: Stellar electron capture rates and the 54Fe(n, p) experiment. Nucl. Phys. A **526**, 161(1991).

Nabi, J.-U, Rahman, M.-Ur-: Gamow-Teller transitions from 24Mg and their impact on the electron capture rates in the O+Ne+Mg cores of stars. Phys. Rev. C **75**, 035803 (2007).

Nabi,J.-U: Weak-Interaction-Mediated Rates on Iron Isotopes for Presupernova Evolution of Massive Stars. Eur. Phys. J. A **40**, 223 (2009).

Nabi,J.-U: Nickel isotopes in stellar matter Eur. Phys. J. A **48**, 84 (2012).

Langanke, K., Martinez-Pinedo, G.: Shell-model calculations of stellar weak interaction rates: II. Weak rates for nuclei in the mass range A=45-65 in supernovae environments. Nucl. Phys. **A673**, 481(2000).

Nabi, J.-U., Klapdor-Kleingrothaus, H.V.: Weak Interaction Rates of sd-Shell Nuclei in Stellar Eenvironments Calculated in the ProtonNeutron Quasiparticle Random-Phase Approximation. At. Data Nucl. Data Tables **71**, 149 (1999).

Dean, D.J., Langanke, K., Chatterjee, L., Radha, P.B., Strayer, M.R.: Electron capture on iron group nuclei. Phys. Rev. C **58**, 536 (1998).

Caurier, E., Langanke, K., Martínez-Pinedo, G., Nowacki, F.: Shell-model calculations of stellar weak interaction rates. I. Gamow-Teller distributions and spectra of nuclei in the mass range A = 4565. Nucl. Phys. A **653(4)**, 439(1999).

Zhi, Q., Langanke, K., Martinez-Pinedo, G., Nowacki, F., Sieja, K.: The 76Se Gamow-Teller strength distribution and its importance for stellar electron capture rates. Nuclear Physics **A859**, 172184 (2011).

Sasano, M., Sakai, H., Yako, K., Wakasa, T., Dozono, M., Rodin, V., Faessler, A., Fujita, K., Greenfield, M. B., Hatanaka, K., Itoh, K., Kawabata, T., Kuboki, H., Maeda, Y., Miki, K., Muto, K., Noji, S., Okamura, H., Sakemi, Y., Sekiguchi, K., Shimizu,Y., Sasamoto, Y., Tameshige, Y., Tamii, A., Uesaka, T.: Gamow-Teller transition strengths in the intermediate nucleus of the 116Cd double- decay by the 116Cd(p, n)116In and 116Sn(n, p)116In reactions at 300 MeV. Phys. Rev. C **85**, 061301(R) (2012).

Heger, A., Woosley, S.E., Martinez-Pinedo, G., Langanke, K.: Presupernova Evolution with Improved Rates for Weak Interactions. Astrophy. J. **560**, 307 (2001).

Fujita, Y., Adachi, T., Brentano, P. von Berg, G. P. A., Fransen, C., De Frenne, D., Fujita, H., Fujita, K., Hatanaka, K., Jacobs, E., Nakanishi, K., Negret, A., Pietralla, N., Popescu, L., Rubio, B., Sakemi, Y., Shimbara, Y., Shimizu, Y., Tameshige, Y., Tamii, A., Yosoi, M., Zell, K. O.: Gamow-Teller strengths in proton-rich exotic nuclei deduced in the combined analysis of mirror transitions. Phys. Rev. Lett. **95**, 212501 (2005).

Aufderheide M. B., Fushiki I., Woosley S. E., Stanford E. and Hartmann D. H.: Search for important weak interaction nuclei in presupernova evolution. Astrophys. J. Suppl. Ser.**91**, 389 (1994).

Nabi J.-U, Johnson C. W.: Comparison of Gamow-Teller strengths in the random phase approximation. J. Phys. G 40, 065202 (2013).

Halbleib, J. A., Sorensen, R. A.: Gamow-Teller beta decay in heavy spherical nuclei and the unlike particle-hole rpa. Nucl. Phys. A **98**, 542 (1967).

Staudt, A., Hirsch, M., Muto, K., Klapdor-Kleingrothaus, H. V.: Calculation of -delayed fission of 180Tl and application of the quasiparticle random-phase approximation to the prediction of β^+- decay half-lives of neutron-deficient isotopes. Phys. Rev. Lett. **65**, 1543 (1990).

Muto, K., Bender, E., Oda, T., Klapdor-Kleingrothaus, H. V.: Proton-neutron quasiparticle RPA with separable Gamow-Teller forces. Z. Phys. A **341**, 407 (1992).

Soloviev, V. G.: Fragmentation of single-particle and collective motions in the quasiparticlephonon nuclear model. Prog. Part. Nucl. Phys. **19**, 107 (1987).

Kuzmin, V. A., Soloviev, V. G.: Gamow-Teller β^+ decays and strength functions of (n, p) transitions in spherical nuclei. Nucl. Phys. A **486**, 118 (1988).

Jokinen, A., Nieminen, A., yst, J., Borcea, R., Caurier, E., Dendooven, P., Gierlik, M., Grska, M., Grawe, H., Hellstrm, M., Karny, M., Janas, Z., Kirchner, R., La Commara, M., Martínez-Pinedo, G., Mayet, P., Penttil, H., Plochocki, A., Rejmund, M., Roeckl, E., Sawicka, M., Schlegel, C., Schmidt, K., Schwengner, R.: Beta decay of 57Zn. Euro. Phys. J. Direct A **3**, 1 (2002).

Osterfeld F.: Nuclear spin and isospin excitations. Rev. Mod. Phys. **64**, 491 (1992).

Gove, N. B., Martin, M. J.: Log-f tables for beta decay. Nucl. Data Tables **10**, 205 (1971).

Bumer, C., Van den Berg, A. M., Davids, B., Frekers, D., De Frenne, D., Grewe, E.-W., Haefner, P., Harakeh, M. N., Hofmann, F., Hunyadi, M., Jacobs, E., Junk, B. C., Korff, A., Langanke, K., Martinez-Pinedo, G., Negret, A., von Neumann-Cosel, P., Popescu, L., Rakers, S., Richter, A., Wrtche, H. J.: High-resolution study of the Gamow-Teller strength distribution in 51Ti measured through 51V(d,2He)51Ti. Phys. Rev. C **68**, 031303(R) (2003).

Jackson,K.P., Celler, A., Alford, W.P., Raywood, K., Abbeg, R., Azuma, R.E., Campbell, C.K., El-Kateb, S., Frekers, D., Green, P.W., Husser, O., Helemer, R., Henderson, R.S., Hicks, K.H., Jeppesen, R., Lewis, P., Miller, G.A., Moalem, A., Moinester, M.A., Schubank, R.B., Shute, G.G., Spicer, B.M., Vetterli, M.C., Yavin, A.I., Yen, S.: The (n, p) Reaction as a Probe of Gamow-Teller Strength. Phys. Lett. B **201**, 25(1988).

Williams, A.L., Alford, W.P., Brash, E., Brown, B.A., Burzynski, S., Fortune, H.T., Husser, O., Helmer, R., Henderson, R., Hui, P.P., Jackson, K.P., Larson, B., McKinzie, M.G., Smith, D.A., Trudel, A., Vetterli, M.: Gamow-Teller strength in 60,62,64Ni(n, p) reactions at 198 MeV. Phys. Rev. C **51**, 11441153 (1995).

Alford, W. P., Brwon, B.A ., Burzynski, S., Celler, A., Frekers, D., Helemer, R., Henderson, R., Jackson, K. P., Lee, K., Rahav, A., Trudel, A. Vetterli, M. C.: Spin-isospin strength distributions in f-p shell nuclei: A study of the 51V(n, p) and 59Co(n, p) reactions at 198 MeV. Phys. Rev. C **48**, 2818 (1993).

Audi, G., Bersillon, O., Blachot, J., Wapstra, A. H.: The NUBASE evaluation of nuclear and decay properties. Nucl. Phys. **A729**, 3 (2003a).

Audi, G., Wapstra, A. H., Thibault, C.: The AME2003 atomic mass evaluation (II): tables, graphs and references. Nucl. Phys. **A729**, 337 (2003b).

Burrows, A., Sawyer, R.F.: Effects of correlations on neutrino opacities in nuclear matter. Phys. Rev. C **58**, 554(1998).

Langanke, K., Martínez-Pinedo, G.: Supernova electron capture rates for Co-55 and Ni-56. Phys. Lett. **B436**, 19(1998).

Poves A., Sánchez-Solano J., Caurier E., and Nowacki F.: Shell model study of the isobaric chains A = 50, A = 51 and A = 52. Nucl. Phys. **A 694**, 157 (2001).

Gao, Z.F., Wang, N., Yuan, J.P., Jiang, L., Song, D.L.: Numerical simulation of the electron capture process in a magnetar interior. Astrophys. Space Sci. **332**, 129-138 (2011).

Gao, Z.F., Peng, Q.H., Wang, N., Chou, C.K., Huo, W.S.: The Landau level-superfluid modified factor and the overall soft X/γ-ray efficiency coefficient of a magnetar. Astrophys. Space Sci. **336**, 427-439 (2011).

Gao, Z.F., Wang, N., Song, D.L., Yuan, J.P., Chou, C.-K.: The effects of intense magnetic fields on Landau levels in a neutron star. Astrophys. Space Sci. **334**, 281-292(2011).

Gao, Z.F., Peng, Q.H., Wang, N., Yuan, J.P.: Magnetic field decay of magnetars in supernova remnants. Astrophys. Space Sci. **342**, 55-71 (2012).

Jing-Jing Liu : MNRAS **433**, 1108-1113 (2013).

Juodagalvis, A., Langanke, K., Hix, W.R., Martinez-Pinedo, G., Sampaio, J.M.: Improved estimate of electron capture rates on nuclei during stellar core collapse. Nucl. Phys. **A 848**,454-478 (2010).

Riper, K.A.V.: Effects of nuclear equation of state on general relativistic stellar core collapse models. The Astrophysical Journal **326**,235-240 (1988).

Bethe H. E.: Supernova Mechanisms. Rev. Mod. Phys. **62**, 801 (1990).

Heeger, A., Woosley, S.E., Martinez-Pinedo, G., Langanke, K.: Presupernova evolution with improved rates for weak interations. The Astrophysical Journal **560**,307-325 (2001).

Umeda, H., Nomoto, K.: Nucleosynthesis of Zinc and Iron peak elements in Population III Type II supernovae: comparison with abundances of very metal poor halo stars. Astrophys. J. **565**,385-404 (2002).

This manuscript was prepared with the AAS LaTeX macros v5.2.

Table 1 Measured and calculated centroids and total GT strengths in electron capture direction for odd-A nuclei. The references are: (a) → (39), (b) → (21), (c) → (36), (d) → (39), (e) → (44).

Nucleus	Model	E(GT_+) MeV	$\sum B(GT_+)$ arb. units
^{59}Co			
	EXP[a]	4.4 ± 0.3	1.9 ± 0.1
	pn-QRPA	5.60	3.32
	SM[b]	5.05	2.50
	Ref. (1)	-	2.4 ± 0.3
	Ref. (3)	2.00	-
^{51}V			
	EXP[c]	4.1 ± 0.4	0.9 ± 0.1
	EXP[d]	-	1.2 ± 0.1
	pn-QRPA	4.20	0.79
	SM[e]	4.34	-
	SM[b]	5.18	1.4
	Ref. (1)	-	1.5 ± 0.2
	Ref. (3)	3.83	-

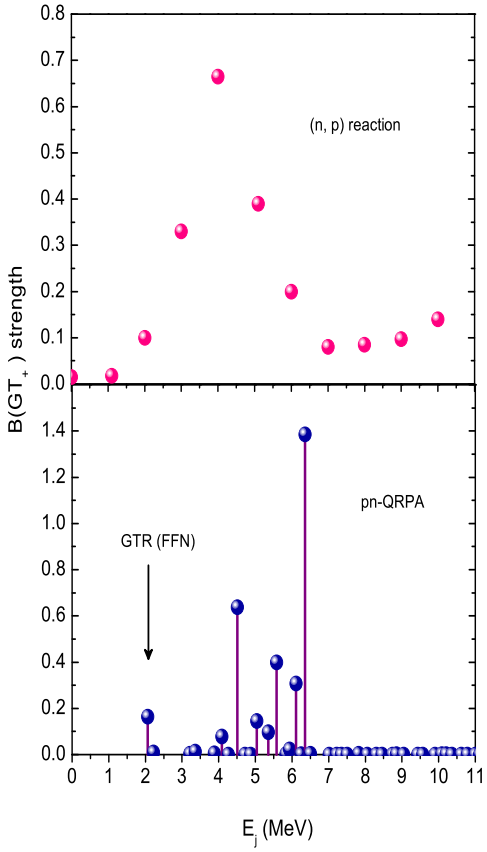

Fig. 1 B(GT_+) strength distributions for ^{59}Co as function of excitation energy in ^{59}Fe. The upper panel depicts result of the (n, p) reaction experiment (39) whereas the lower panel shows the pn-QRPA calculation (present work). The arrow denotes the placement of the centroid of the GT resonance predicted by FFN (3; 4).

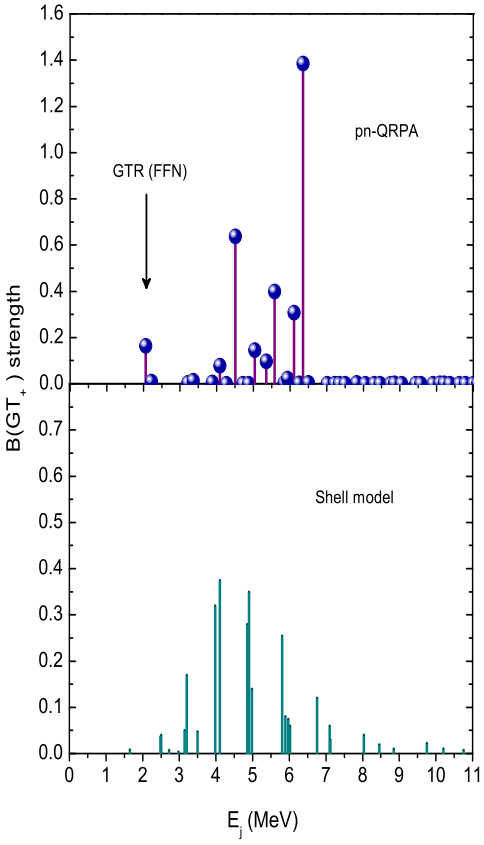

Fig. 2 B(GT_+) strength distributions for ^{59}Co as function of excitation energy in ^{59}Fe. The upper panel depicts the pn-QRPA calculation (present work) whereas the lower panel shows the shell model (21) results. The arrow denotes the placement of the centroid of the GT resonance predicted by FFN (3; 4).

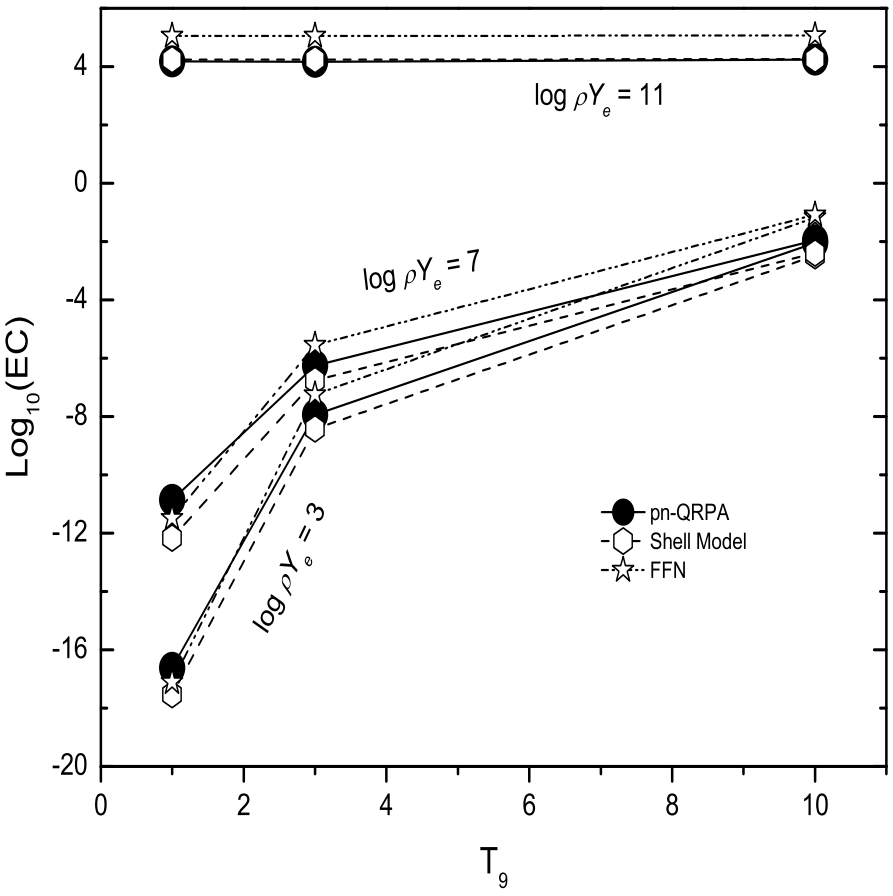

Fig. 3 Comparison of the pn-QRPA, large scale shell model (18), and FFN (3; 4) stellar electron capture rate calculations on ^{59}Co as a function of stellar temperature for selected densities. For units see text.